Original

Froebel, U.:

Hot-Workability of Gamma-Based TiAl Alloys during Severe Deformation

In: Materials Science Forum, THERMEC 2009 (2010) Trans Tech Publications

DOI: 10.4028/www.scientific.net/MSF.638-642.1300

Materials Science Forum *Online: 2010-01-12*
ISSN: 1662-9752, Vols. 638-642, pp 1300-1305
doi:10.4028/www.scientific.net/MSF.638-642.1300

Hot-Workability of Gamma-Based TiAl Alloys during Severe Deformation

U. Froebel

GKSS Research Centre, Institute of Materials Research, Max-Planck-Straße 1, D-21502 Geesthacht, Germany
ulrich.froebel@gkss.de

Keywords: Titanium Aluminides; Hot-Working; Severe Deformation; Shear Localization; Recovery

Abstract

Forged and extruded TiAl products suffer from structural and chemical inhomogeneities that reduce the reliability of components. In an attempt to improve the homogeneity of the material, the feasibility of cyclic axial deformation and cyclic torsional deformation superimposed with compression, where much higher strains can be imparted into the material than during forging and extrusion, were investigated. Accordingly, during torsion superimposed with compression pronounced shear localization and cracking occurs. These difficulties can largely be overcome by cyclic axial deformation.

Introduction

Gamma-based Titanium aluminides are intrinsically brittle up to relatively high temperatures. Inhomogeneous microstructures are particularly harmful in this respect because critical values of constraint stress can develop after small strain, leading to premature failure of the material. The chemical and structural homogeneity of components is hence extremely important for engineering applications and can most effectively be accomplished by thermomechanical processing. The associated degree of microstructural transformation is determined by the imparted energy, which triggers dynamic recrystallization. During traditional metal-forming processes such as forging and extrusion, the strain and thus the imparted energy is inevitably limited due to geometrical constraints. This often leads to insufficient material consolidation, which is manifested by incomplete recrystallization and significant chemical inhomogeneity. Considerably increasing the deformation strain is therefore necessary to improve the homogeneity of components. In this context the feasibility of cyclic torsional deformation combined with compression and cyclic axial deformation was investigated. Cyclic axial deformation means that the sample is alternately deformed in tension and compression, whereas during cyclic torsional deformation the turning direction is reversed after relatively small twist angles. During torsion superimposed with compression pronounced shear localization and cracking occurs impeding the material consolidation by dynamic recrystallization. In comparison, the liability to shear localization and cracking is far less pronounced during cyclic axial deformation so that recrystallization is mainly limited by strain-rate sensitive recovery processes. In the following both the shear localization which occurs during torsion and the competing grain refinement and recovery processes during cyclic axial deformation will be addressed.

Experimental procedure

The hot-working experiments were conducted on two γ-based alloys with the compositions Ti-45Al-5Nb and Ti-46.5Al-5Nb. These alloys fall within the so-called high niobium containing group of TiAl alloys, which are currently being investigated for engineering applications [1]. The two materials were supplied by the Flow Serve Corp. as induction skull melted and HIPed (hot isostatically pressed at 1185°C and 172MPa for 4hrs) ingots of 70mm diameter and 1000mm length. The specimens were prepared by spark erosion, turning, and drilling.
The microstructures were analyzed with the scanning electron microscope (SEM) Leo Gemini 1530. The SEM samples were prepared by grinding and electropolishing or alternately by vibratory polishing (Vibromet 2 from the Buehler Corp.) For the transmission electron microscope (TEM) observations, 0.5mm thick slices were cut from the longitudinal section through the central axis of

the sample, ground to 100μm thickness, and then thinned to electron transparency by twin jet polishing. The thin foils were examined with a PHILLIPS electron microscope CM200.
Hot-working was partly performed in a servohydraulic hot torsion testing machine (Gleeble 3500/3800). The details are described elsewhere [2]. Cyclic axial deformation experiments were also conducted in a universal servohydraulic testing machine (MTS 810) with the displacement used as a feed-back parameter. This machine can impart much higher stresses than the torsion testing machine. High yield stresses can arise in TiAl alloys at deformation temperatures around 1200°C. These result from the high strain-rates that are necessary to minimize recovery processes and the high strain-rate sensitivity of the material at such high temperatures. The samples had a diameter of 10mm and a length of 120mm. Both ends were threaded so that they could be fixed into the water-cooled grips and a counter nut was used to prevent any play movement. The samples were induction heated within a length of 5mm. The temperature was controlled with an optical pyrometer, which was calibrated with the aid of Pt/Pt-Rd thermocouples that were spot welded onto a calibration sample.

Cyclic torsional deformation with superimposed compression

During torsion the strain increases linearly with the radial distance from the sample axis (Figure 1a). To generate a more homogeneous deformation state, a compressive stress was superimposed with torsion (Figure 1a) so that the major shear processes intersect. Yet the material deforms very inhomogeneously during severe torsional deformation at temperatures around 1200°C [2], which is manifested by narrow shear bands and cracking (Figures 1b and 1c). The mechanisms that underlie these phenomena were analyzed in detail in a recent study [2]. According to these investigations, preliminary forms of shear bands are the kink bands shown in Figure 1c (arrow 1). Kink bands develop when the lamellae bend beyond a critical value under the combined influence of torsion and compression. The lamellae become then separated by dynamic recrystallization. The regions where the lamellae separate are preferred sites for the formation of very fine grains (arrow 1 of Figure 1c) providing a high density of additional grain boundaries that can act as further sites for recrystallization. The deformation of such grains may consequently lead to intensive recrystallization. The recrystallization processes result in a thickening of the buckled interfaces at the expense of the adjacent lamellae so that eventually a shear band is formed. The deformation concentration leads to extremely high strains within the shear band. In the course of deformation voids develop at places where the transfer of deformation is difficult. Growth and coalescence of the voids, as seen in front of the upper crack tip in Figure 1c (arrow 2) leading to a complete separation of the material in a later state of deformation.

Cyclic axial deformation

Figure 2a shows the microstructure of alloy Ti-45Al-5Nb in the as-cast and HIPed state. The microstructure is dominantly lamellar with colony sizes of approximately 400μm and minor amounts of small grains at the colony boundaries. During cyclic axial deformation (Figure 2b) the material deforms much more homogeneously than during torsional deformation (Figure 2c). In view of the very high strain of ε=1200%, however, the degree of microstructure transformation is small when compared with the as-cast and HIPed state (compare Figures 2a and 2d). The amount of grains at the colony boundaries slightly increased but the colonies did not refine. The lamellae became only coarser and buckled in some regions (arrow in Figure 2d). It may thus be suggested that the material underwent recovery.
To obtain evidence for this assumption, the dislocations in the hot-worked material were examined with regard to configurations being characteristic for recovery processes. The examinations were confined to the defect structures within the γ(TiAl) phase, which is a major microstructural constituent of the alloys. Because of the ordered structure of the γ phase (Figure 3a) deformation is carried by 1/2<110] and <001> ordinary dislocations as well as by <011] and 1/2<112] superdislocations [3].
The weak beam images of Figures 3b and 3c indicate the dislocation structure in a γ grain. There are ordinary dislocations and superdislocations present. The ordinary dislocations often tend to align parallel to each other as indicated in Figure 3b. Through diffraction contrast experiments the segments were identified as ordinary dislocations in edge orientation (Figure 3c). Whether they are ordinary dislocations of the 1/2<110] or <100] type, however, is not entirely clear because both types of dislocations are invisible under the (001) reflection used in Figure 3c. <100] dislocations were found to contribute to deformation at temperatures above 1000°C [4]. But the dislocations

become metastable and decompose into 1/2<110] dislocations during cooling [4]. Because no such decomposition was observed it might be concluded that the segments are 1/2<110] dislocations. The segments in the γ lamellae of Figure 3d were unambiguously identified as 1/2<110] ordinary dislocations. They are again aligned almost parallel to each other showing a pronounced edge orientation. According to these findings the ordinary dislocations tend to form small-angle grain boundaries at deformation temperatures of about 1120°C and strain-rates around $\dot{\varepsilon}=10^{-2}s^{-1}$ by glide and diffusion assisted climb processes as schematically drawn in Figure 3e. The formation of the small angle grain boundaries reduces the lattice distortion energy, which results from the stress fields of the dislocations, and consequently the imparted energy that can trigger dynamic recrystallization.

To reduce recovery processes and obtain a more complete transformation of the as-cast and HIPed morphology, the strain-rates were thus increased considerably. Figure 4a indicates the microstructure after deformation at 1120°C and a strain-rate of $\dot{\varepsilon}=10^{-1}s^{-1}$. Under these conditions the material underwent a complete microstructure transformation resulting in an average colony size of about 100μm (compare Figures 2a and 4a). The microstructure is, however, still dominantly lamellar. Globular microstructures can be achieved at this temperature only at strain-rates of about $\dot{\varepsilon}=0.5s^{-1}$, as indicated in Figure 4b.

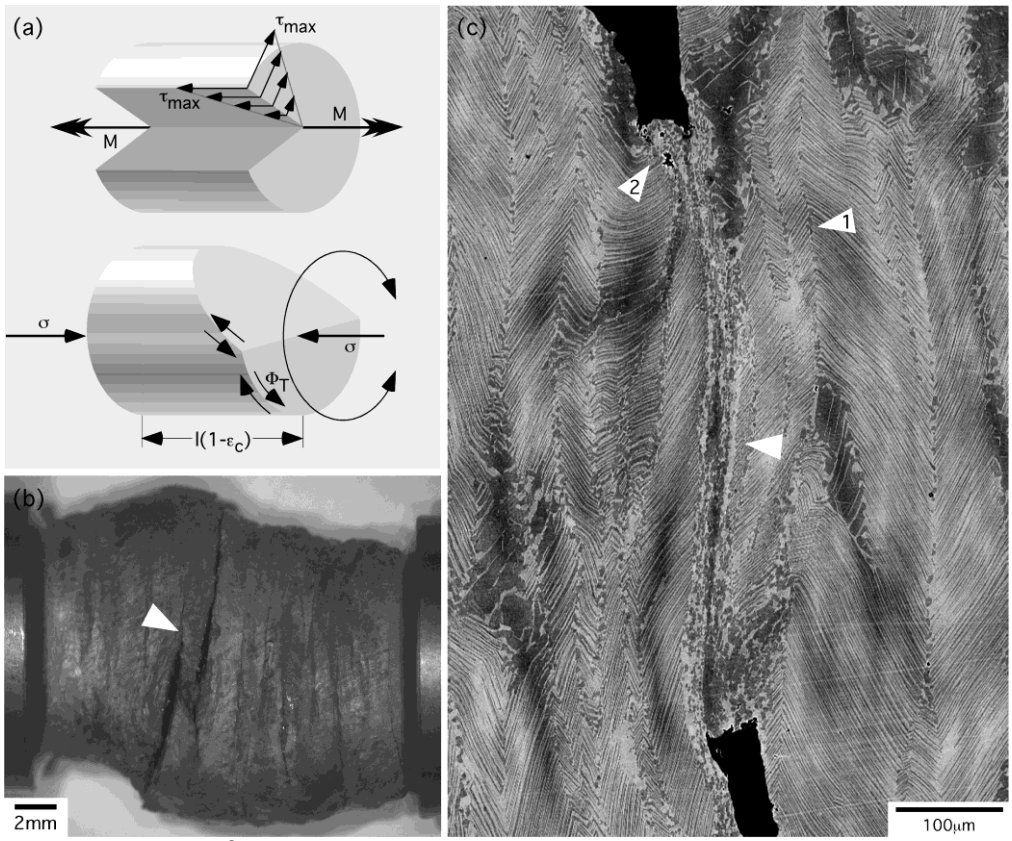

Fig. 1. Cyclic torsional deformation combined with compression. (a). Schematic drawing of the shear components τ in a cylindrical bar subjected to a torque M. During torsion combined with compression the imparted strain is composed of the torsional shear strain $\Phi_T=r\cdot\theta/l$ (r is the radius, θ the twist angle in radians, and l the gauge length) and the compressive strain ε_c. (b) Failure during severe torsional deformation combined with compression. Side view. Ti-46.5Al-5Nb, T=1200°C, Φ_T(torsion direction reversed after 1/8 revolution)=9.3, $\dot{\Phi}_T=1.7\cdot10^{-3}s^{-1}$, ε=0.28. (c) Backscattered electron (BSE) image showing a part of the central crack (marked by an arrow in (b)) in the longitudinal section of the sample. The shear band is marked by an arrow. There are several kink bands parallel to the shear band decorated with fine grains (arrow 1). Note also the coalesced voids in front of the upper crack tip (arrow 2).

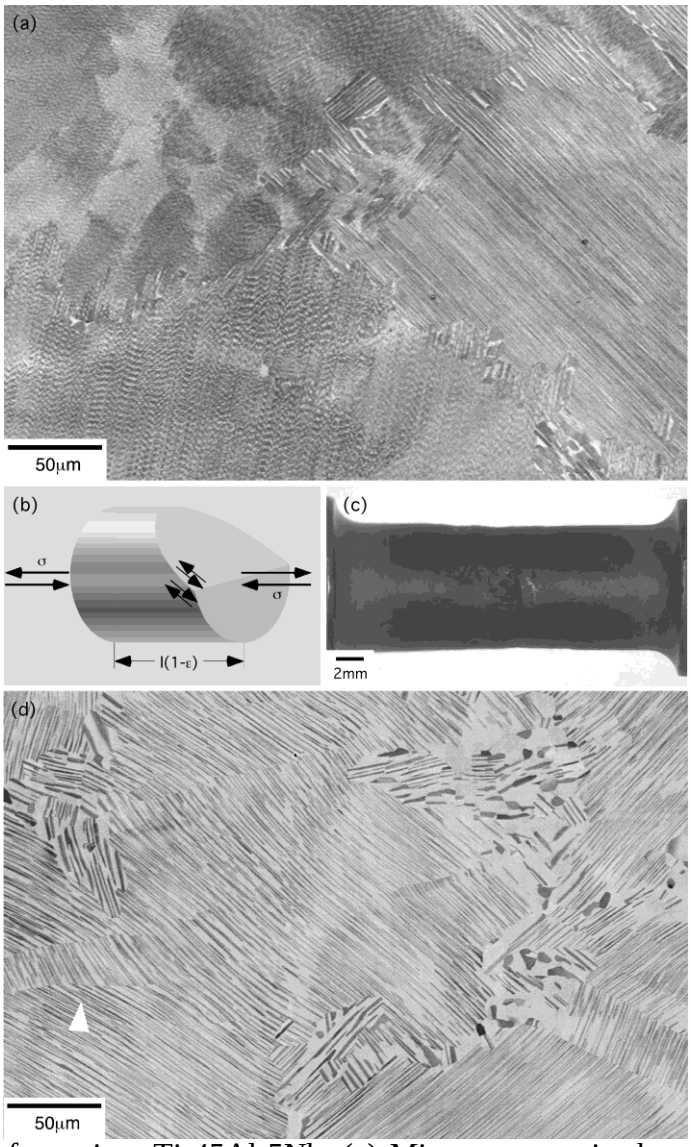

Fig. 2. Cyclic axial deformation. Ti-45Al-5Nb. (a) Microstructure in the as-cast and HIPed state. The microstructure is dominantly lamellar. (b) Schematic drawing of cyclic axial deformation that consists of alternating deformation in tension and compression. (c) Homogeneous deformation during severe cyclic axial deformation. T=1120°C, ε=12, $\dot{\varepsilon}$=$5\cdot10^{-3}s^{-1}$. (d) Resulting microstructure shown in the longitudinal section of the sample. Note the buckled lamellae (arrow).

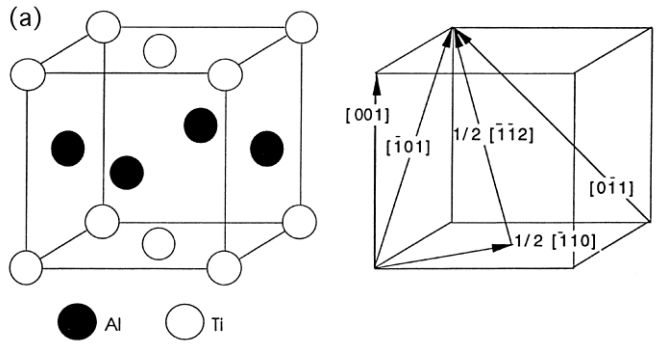

Fig. 3. Dislocation structure during severe cyclic axial deformation. (a) Atomic arrangement in the ordered face centred tetragonal $L1_0$ structure of γ(TiAl) and the Burgers vectors of 1/2<110] and <001> ordinary dislocations as well as 1/2<112] and <011] superdislocations.

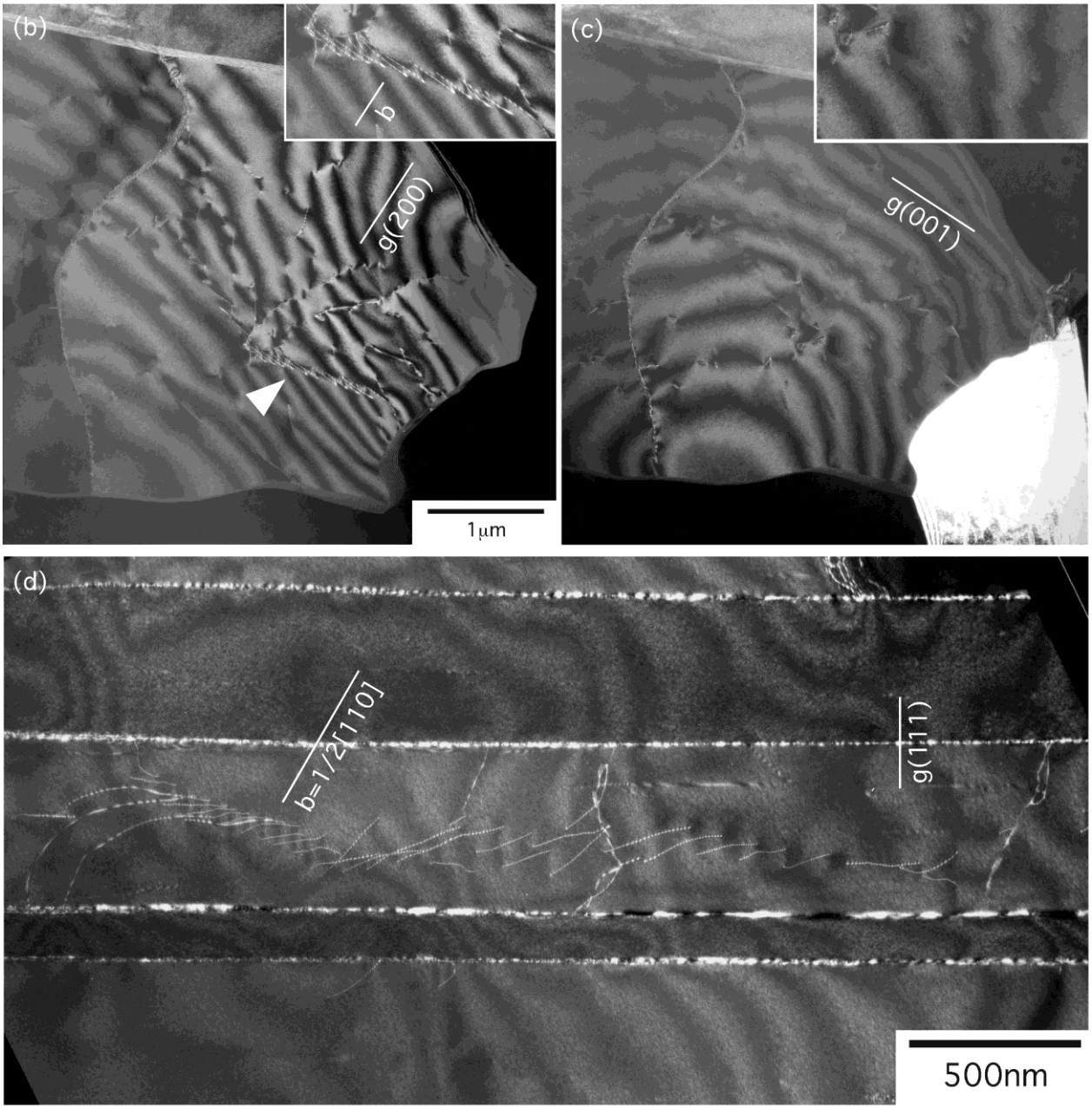

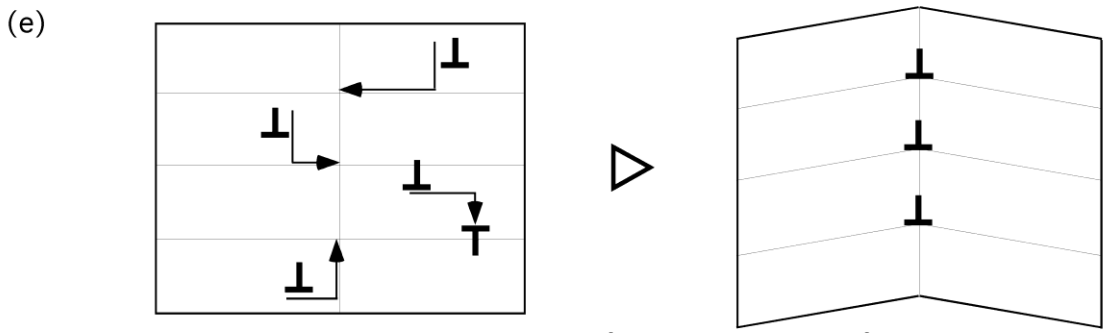

Fig. 3 (continuation). (b) Weak beam image of an arrangement of parallel dislocation segments (arrow) in a γ grain that is shown in the insert in higher magnification using the g=(200) reflection. Ti-45Al-5Nb, T=1120°C, ε=12, $\dot{\varepsilon}=5\cdot10^{-3}s^{-1}$. (c) The dislocations are not visible when using the g=(001) reflection thereby indicating that they are ordinary dislocations in edge orientation. Foil orientation close to [010]. (d) Parallel arrangement of 1/2<110] ordinary dislocations in a γ lamellae showing pronounced edge orientation. Foil orientation close to [$\bar{2}$11]. (e) Schematic drawing of a small-angle grain boundary formed by glide and climb processes.

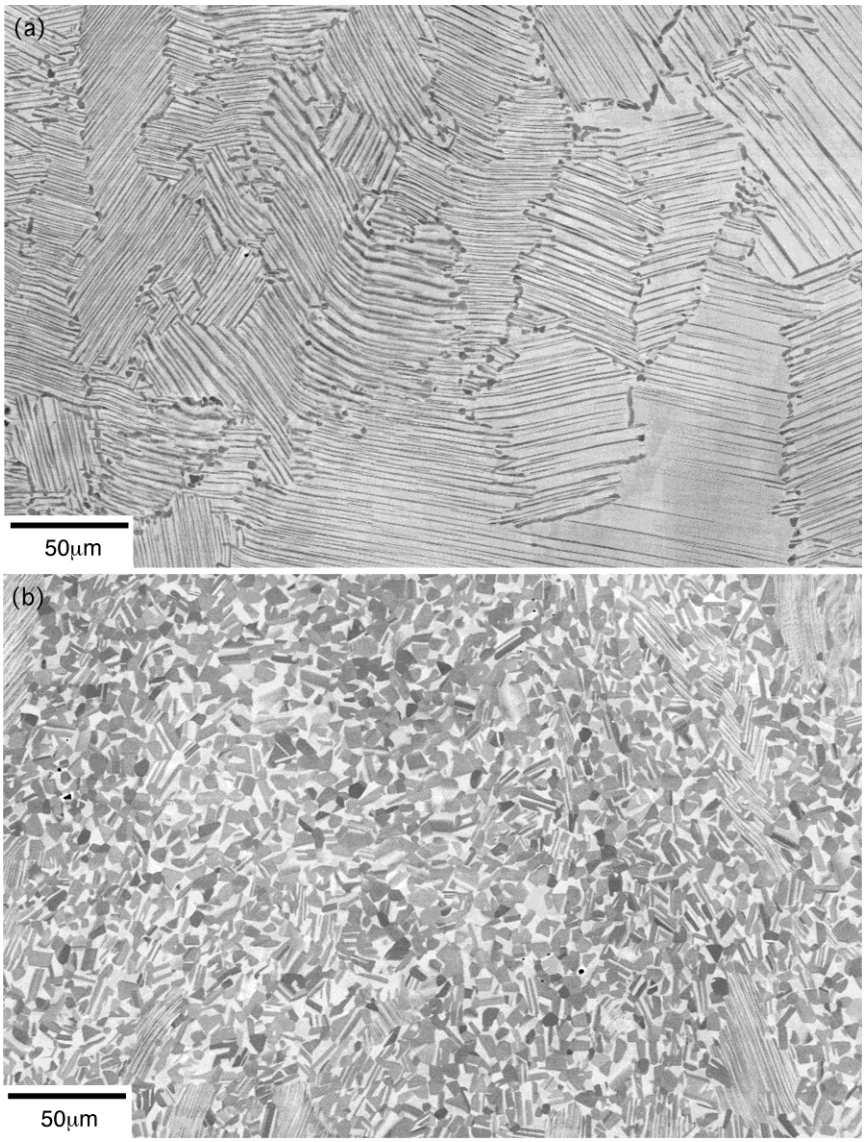

Fig. 4. Cyclic axial deformation. Ti-45Al-5Nb. (a) Microstructure after deformation at a strain-rate of $\dot{\varepsilon}=10^{-1}s^{-1}$. T=1120°C, ε=18. (b) Microstructure after deformation at a strain-rate of $\dot{\varepsilon}=3.2\cdot10^{-1}s^{-1}$. T=1120°C.

Conclusions

Primary hot-working processes are determined by the plastic anisotropy of the lamellar structure, which is the major microstructural constituent of TiAl alloys in the as-cast and HIPed state. During cyclic torsion with superimposed compression at 1200°C the anisotropy leads to pronounced shear localization preventing a global refinement of the material by dynamic recrystallization. This can largely be overcome by using cyclic axial deformation. Grain refinement is predominantly limited by recovery processes. These processes can be suppressed at temperatures around 1100°C by using strain-rates exceeding $\dot{\varepsilon}=10^{-1}s^{-1}$. Ongoing work will optimize the hot-working parameters to obtain a completely transformed globular microstructure that is suitable for secondary processing.

References

[1] F. Appel, M. Oehring, and R. Wagner: Intermetallics Vol. 8 (2000), p. 1283.
[2] U. Froebel and F. Appel: Metall Mater Trans A Vol. 38A (2007), p. 1817.
[3] M. Yamaguchi and Y. Umakoshi: Prog Mater Sci Vol. 34 (1990), p. 1.
[4] S. H. Whang and Y. D. Hahn: Scipta metal Mater Vol. 24 (1990), p. 1679.